Composites: Part B 47 (2013) 8–25

Contents lists available at SciVerse ScienceDirect

Composites: Part B

journal homepage: www.elsevier.com/locate/compositesb

Maximization of fundamental frequency of axially compressed laminated curved panels with cutouts

Hsuan-Teh Hu *, Hung-Wei Peng

Department of Civil Engineering and Sustainable Environment Research Center, National Cheng Kung University, Tainan 701, Taiwan, ROC

ARTICLE INFO

Article history:
Received 5 October 2011
Received in revised form 28 August 2012
Accepted 29 October 2012
Available online 29 November 2012

Keyword:
C. Finite element analysis

ABSTRACT

Free vibration analyses of laminated curved panels with central circular cutouts and subjected to axial compressive forces are carried out by employing the Abaqus finite element program. The fundamental frequencies of these composite laminated curved panels with a given material system are then maximized with respect to fiber orientations by using the golden section method. Through parametric studies, the significant influences of the panel aspect ratio, the panel curvature, the cutout size and the compressive force on the maximum fundamental frequencies, the optimal fiber orientations and the associated fundamental vibration modes of these panels are demonstrated and discussed.

1. Introduction

The applications of fiber-composite laminate materials to aerospace industrial such as spacecraft, high-speed aircraft and satellite have increased rapidly in recent years. The most major components of the aerospace structures are frequently made of curved panels with cutouts and subjected to various kinds of compressive forces. Therefore, knowledge of the dynamic characteristics of composite laminated curved panels with cutouts in compression, such as their fundamental natural frequency, is essential.

The fundamental natural frequency of composite laminated curved panels highly depends on the ply orientations [1–9], geometries [2,3,6–9], cutouts [6,9–15] and compressive forces [9,16–19]. Therefore, proper selection of appropriate lamination to maximize the fundamental frequency of composite laminated curved panels with central cutout in compression becomes a crucial problem [4,20–22].

Research on the subject of structural optimization has been reported by many investigators [23] and has been widely employed to study the dynamic behavior of composite structures [6,7–9,12,21,22,24,25]. Among various optimization schemes, the golden section method is a simple technique and can be easily programmed for solution on the computer [26,27]. Up to now, most of the investigations are dealt with the frequency optimization for structural components with no initial stress. Only little research has been done on the frequency optimization for structural components with initial stress [28], not to mention the structural components with cutouts. To fill the gap, maximization of the fundamental natural frequency of simply supported composite laminated curved panels with cutout and in compression is performed in this investigation. The optimization scheme used in this study is the golden section method. The fundamental frequencies of the composite laminated curved panels are calculated by using the Abaqus finite element program [29]. In the paper, the constitutive equations for fiber-composite laminae, vibration analysis and golden section method are briefly reviewed. The influences of the panel aspect ratio, the panel curvature, the cutout size and the compressive force on the maximum fundamental natural frequencies, the optimal fiber orientations and the associated fundamental vibration modes of the laminated curved panels are presented and important conclusions obtained from the study are given.

2. Constitutive matrix for fiber-composite laminae

In the finite element analysis, the laminated cylindrical shells are modeled by eight-node isoparametric shell elements with six degrees of freedom per node (three displacements and three rotations). The reduced integration rule together with hourglass stiffness control is employed to formulate the element stiffness matrix [29].

During the analysis, the constitutive matrices of composite materials at element integration points must be calculated before the stiffness matrices are assembled from element level to global level. For fiber-composite laminate materials, each lamina can be considered as an orthotropic layer. Let $\{\sigma\} = \{\sigma_x, \sigma_y, \tau_{xy}\}^T$, $\{\tau\} = \{\tau_{xz}, \tau_{yz}\}^T$, $\{\varepsilon\} = \{\varepsilon_x, \varepsilon_y, \gamma_{xy}\}^T$ and $\{\gamma\} = \{\gamma_{xz}, \gamma_{yz}\}^T$ be the stresses and strains in the element coordinates (x,y,z) as shown in Fig. 1. The constitutive equations for the lamina at an element integration point can be written as:

$$\{\sigma\} = [T_1]^T[Q_1'][T_1]\{\varepsilon\} = [Q_1]\{\varepsilon\}, \quad \{\tau\} = [T_2]^T[Q_2'][T_2]\{\gamma\} = [Q_2]\{\gamma\} \tag{1}$$

* Corresponding author.
E-mail address: hthu@mail.ncku.edu.tw (H.-T. Hu).

1359-8368/$ - see front matter
http://dx.doi.org/10.1016/j.compositesb.2012.10.047

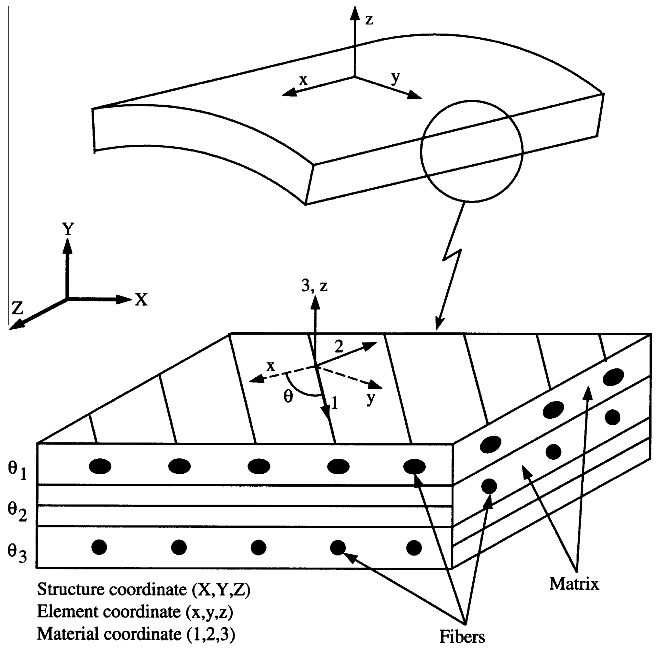

Fig. 1. Material, element and structure coordinates of fiber-composite laminated curved panel.

$$[Q'_1] = \begin{bmatrix} \frac{E_{11}}{1-\nu_{12}\nu_{21}} & \frac{\nu_{12}E_{22}}{1-\nu_{12}\nu_{21}} & 0 \\ \frac{\nu_{21}E_{11}}{1-\nu_{12}\nu_{21}} & \frac{E_{22}}{1-\nu_{12}\nu_{21}} & 0 \\ 0 & 0 & G_{12} \end{bmatrix} \qquad [Q'_2] = \begin{bmatrix} \alpha_1 G_{13} & 0 \\ 0 & \alpha_2 G_{23} \end{bmatrix} \tag{2}$$

$$[T_1] = \begin{bmatrix} \cos^2\theta & \sin^2\theta & \sin\theta\cos\theta \\ \sin^2\theta & \cos^2\theta & -\sin\theta\cos\theta \\ -2\sin\theta\cos\theta & 2\sin\theta\cos\theta & \cos^2\theta - \sin^2\theta \end{bmatrix}, \quad [T_2] = \begin{bmatrix} \cos\theta & \sin\theta \\ -\sin\theta & \cos\theta \end{bmatrix} \tag{3}$$

The α_1 and α_2 in Eq. (2) are shear correction factors, which are calculated in Abaqus by assuming that the transverse shear energy through the thickness of laminate is equal to that in unidirectional bending [29,30]. The fiber orientation θ in Eq. (3) is measured counterclockwise from the element local x-axis to the material 1-axis (Fig. 1).

Let $\{\varepsilon\}_o = \{\varepsilon_{xo}, \varepsilon_{yo}, \varepsilon_{xyo}\}^T$ be the in-plane strains at the mid-surface of the laminate section, $\{\kappa\} = \{\kappa_x, \kappa_y, \kappa_{xy}\}^T$ the curvatures, and h the total thickness of the section. If there are n layers in the laminate section, the stress resultants, $\{N\} = \{N_x, N_y, N_{xy}\}^T$, $\{M\} = \{M_x, M_y, M_{xy}\}^T$ and $\{V\} = \{V_x, V_y\}^T$, can be defined as

$$\begin{Bmatrix} \{N\} \\ \{M\} \\ \{V\} \end{Bmatrix} = \int_{-h/2}^{h/2} \begin{Bmatrix} \{\sigma\} \\ z\{\sigma\} \\ \{\tau\} \end{Bmatrix} dz = \sum_{j=1}^{n} \begin{bmatrix} (z_{jt} - z_{jb})[Q_1] & \frac{1}{2}(z_{jt}^2 - z_{jb}^2)[Q_1] & [0] \\ \frac{1}{2}(z_{jt}^2 - z_{jb}^2)[Q_1] & \frac{1}{3}(z_{jt}^3 - z_{jb}^3)[Q_1] & [0] \\ [0]^T & [0]^T & (z_{jt} - z_{jb})[Q_2] \end{bmatrix} \times \begin{Bmatrix} \{\varepsilon_o\} \\ \{\kappa\} \\ \{\gamma\} \end{Bmatrix} \tag{4}$$

The z_{jt} and z_{jb} are the distance from the mid-surface of the section to the top and the bottom of the jth layer respectively. The [0] is a 3 by 2 matrix with all the coefficients equal to zero.

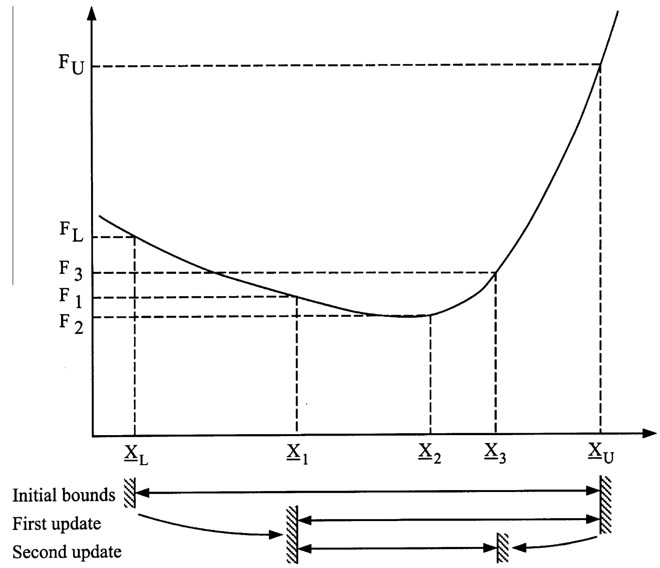

Fig. 2. The golden section method.

3. Vibration analysis

For the free vibration analysis of an undamped structure subjected to initial stresses, the equation of motion of the structure can be written in the following form [31]:

$$[M]\{\ddot{D}\} + ([K]_L + [K]_\sigma)\{D\} = \{0\} \tag{5}$$

where $\{D\}$ is a vector for the unrestrained nodal degrees of freedoms, $\{\ddot{D}\}$ an acceleration vector, $[M]$ the mass matrix of the structure, $[K_L]$ the traditional linear stiffness matrix of the structure, $[K_\sigma]$ a geometric stress stiffness matrix due to the initial stresses and $\{0\}$ a zero vector. Since $\{D\}$ undergoes harmonic motion, we can express

$$\{D\} = \{\bar{D}\}\sin\omega t; \qquad \{\ddot{D}\} = -\omega^2\{\bar{D}\}\sin\omega t \tag{6}$$

where $\{\bar{D}\}$ vector contains the amplitudes of $\{D\}$ vector. Then Eq. (5) can be written in an eigenvalue expression as

$$([K_L] + [K_\sigma] - \omega^2[M])\{\bar{D}\} = \{0\} \tag{7}$$

The preceding equation is an eigenvalue expression. If $\{\bar{D}\}$ is not a zero vector, we must have

$$\left|[K_L] + [K_\sigma] - \omega^2[M]\right| = 0 \tag{8}$$

In Abaqus, a subspace iteration procedure [29] is used to solve for the natural frequency ω, and the eigenvectors (or vibration modes) $\{\bar{D}\}$. The obtained smallest natural frequency (fundamental frequency) is then the objective function for maximization.

4. Golden section method

We begin by presenting the golden section method [26,27] for determining the minimum of the unimodal function F, which is a function of the independent variable $\underline{X}$. It is assumed that lower bound $\underline{X}_L$ and upper bound $\underline{X}_U$ on $\underline{X}$ are known and the minimum can be bracketed (Fig. 2). In addition, we assume that the function has been evaluated at both bounds and the corresponding values are F_L and F_U. Now we can pick up two intermediate points $\underline{X}_1$ and $\underline{X}_2$ such that $\underline{X}_1 < \underline{X}_2$ and evaluate the function at these two points to provide F_1 and F_2. Because F_1 is greater than F_2, now $\underline{X}_1$ forms a new lower bound and we have a new set of bounds, $\underline{X}_1$ and $\underline{X}_U$. We can now select an additional point, $\underline{X}_3$, for which we evaluate F_3. It is clear that F_3 is greater than F_2, so $\underline{X}_3$ replace $\underline{X}_U$

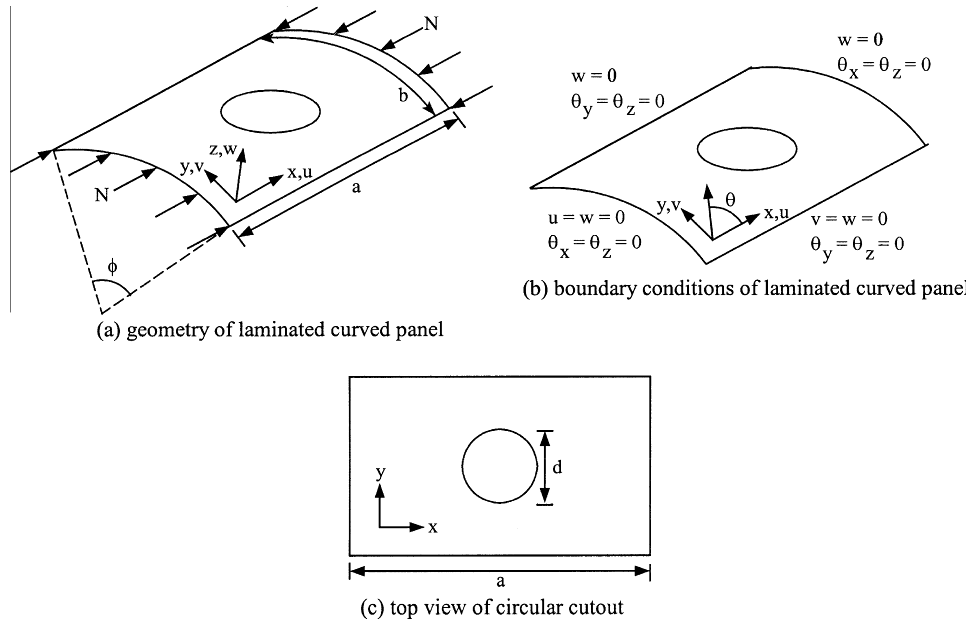

Fig. 3. Geometry of simply supported laminated curved panel with central circular cutout.

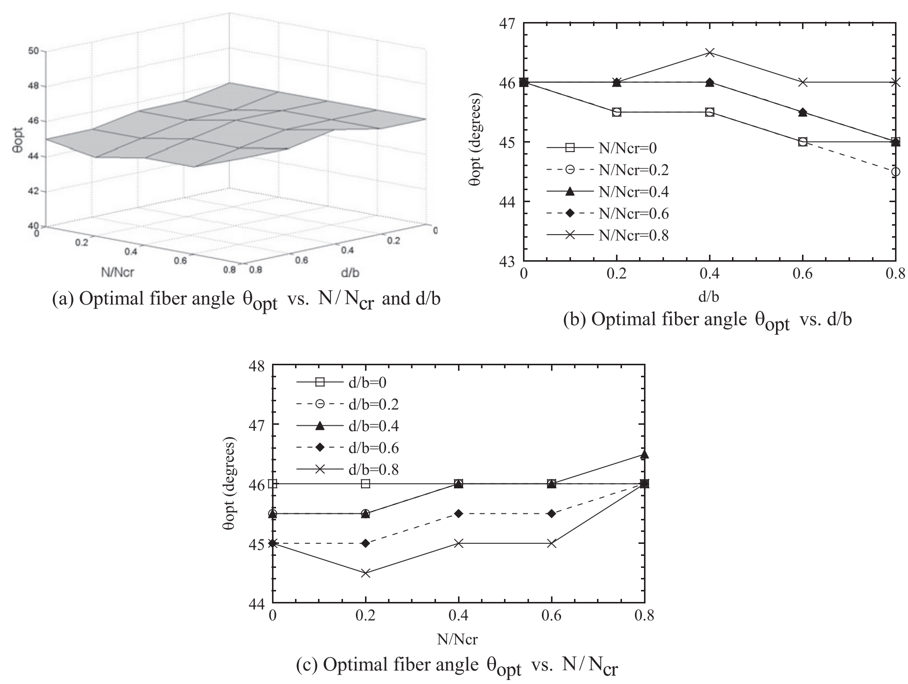

Fig. 4. Effect of cutout size and in-plane compressive force on optimal fiber angle of $[\pm\theta/90/0]_{2s}$ simply supported laminated curved panels with central circular cutout (b = 10 cm, a/b = 1, ϕ = 5°).

as the new upper bound. Repeating this process, we can narrow the bounds to whatever tolerance is desired.

To determine the method for choosing the interior points $\underline{X}_1,\underline{X}_2,\underline{X}_3,\ldots$, we pick the values of $\underline{X}_1$ and $\underline{X}_2$ to be symmetric about the center of the interval and satisfying the following expressions:

$$\underline{X}_U - \underline{X}_2 = \underline{X}_1 - \underline{X}_L \tag{9}$$

$$\frac{\underline{X}_1 - \underline{X}_L}{\underline{X}_U - \underline{X}_L} = \frac{\underline{X}_2 - \underline{X}_1}{\underline{X}_U - \underline{X}_1} \tag{10}$$

Let τ be a number between 0 and 1. We can define the interior points $\underline{X}_1$ and $\underline{X}_2$ to be

$$\underline{X}_1 = (1-\tau)\underline{X}_L + \tau\underline{X}_U \tag{11a}$$

$$\underline{X}_2 = \tau\underline{X}_L + (1-\tau)\underline{X}_U \tag{11b}$$

Substituting Eqs. (11a) and (11b) into Eq. (10), we obtain

$$\tau^2 - 3\tau + 1 = 0 \tag{12}$$

Solving the above equation, we obtain τ = 0.38197. The ratio $(1-\tau)/\tau$ = 1.61803 is the famous “golden section” number. For a problem involving the estimation of the maximum of a one-variable function F, we need only minimize the negative of the function, that is, minimize $-F$.

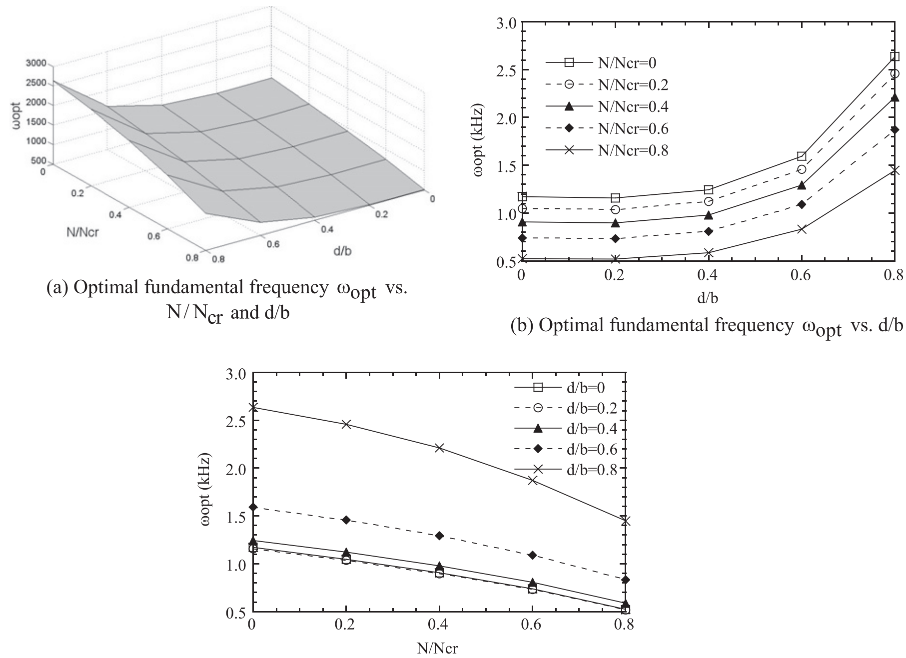

(a) Optimal fundamental frequency ω_{opt} vs. N/N_{cr} and d/b

(b) Optimal fundamental frequency ω_{opt} vs. d/b

(c) Optimal fundamental frequency ω_{opt} vs. N/N_{cr}

Fig. 5. Effect of cutout size and in-plane compressive force on optimal fundamental frequency of $[\pm\theta/90/0]_{2s}$ simply supported laminated curved panels with central circular cutout (b = 10 cm, a/b = 1, ϕ = 5°).

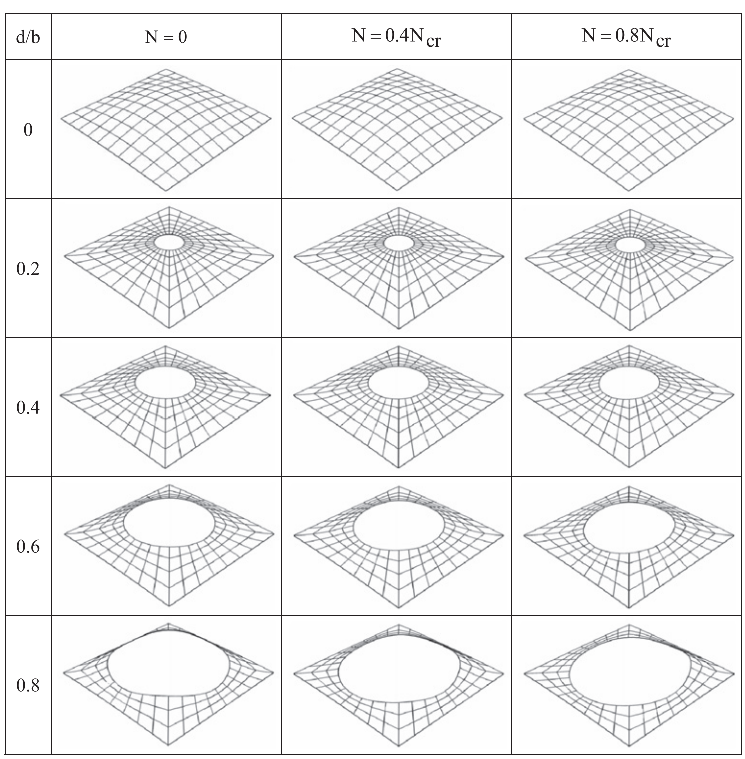

Fig. 6. Fundamental vibration modes of $[\pm\theta/90/0]_{2s}$ simply supported laminated curved panels with central circular cutout and under optimal fiber angles (b = 10 cm, a/b = 1, ϕ = 5°).

5. Numerical analysis

The accuracy of the eight-node shell element in Abaqus program for frequency analysis has been verified by the authors [9,32] and good agreements are obtained between the numerical results and the analytical solution or experimental data. Hence, it is confirmed that the accuracy of the shell element in Abaqus program is good enough to analyze the vibration behavior of laminated curved panels.

In the following sections, simply supported laminated curved panels with central circular cutouts and subjected to various axial

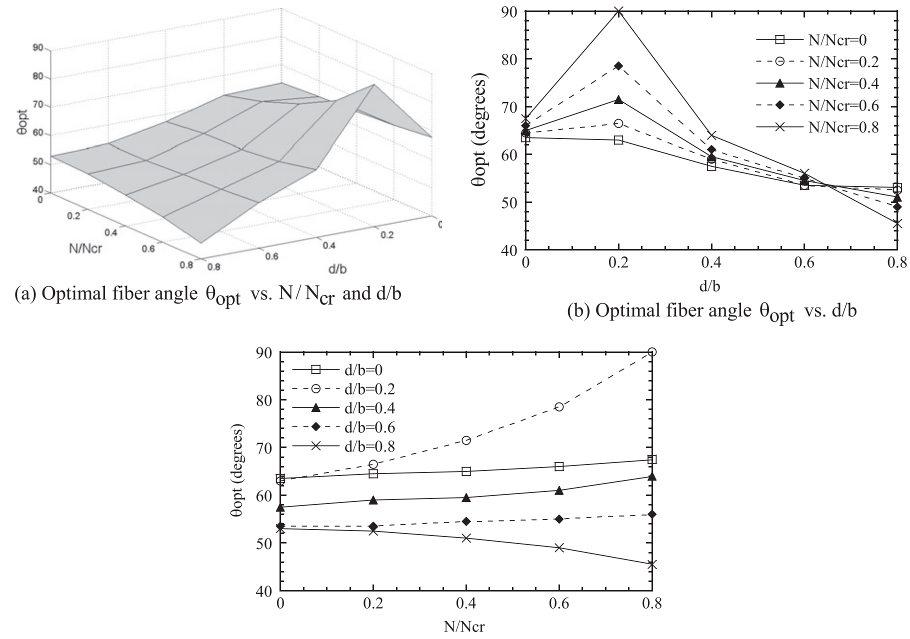

(a) Optimal fiber angle θ_{opt} vs. N/N_{cr} and d/b

(b) Optimal fiber angle θ_{opt} vs. d/b

(c) Optimal fiber angle θ_{opt} vs. N/N_{cr}

Fig. 7. Effect of cutout size and in-plane compressive force on optimal fiber angle of $[\pm\theta/90/0]_{2s}$ simply supported laminated curved panels with central circular cutout (b = 10 cm, a/b = 1, ϕ = 60°).

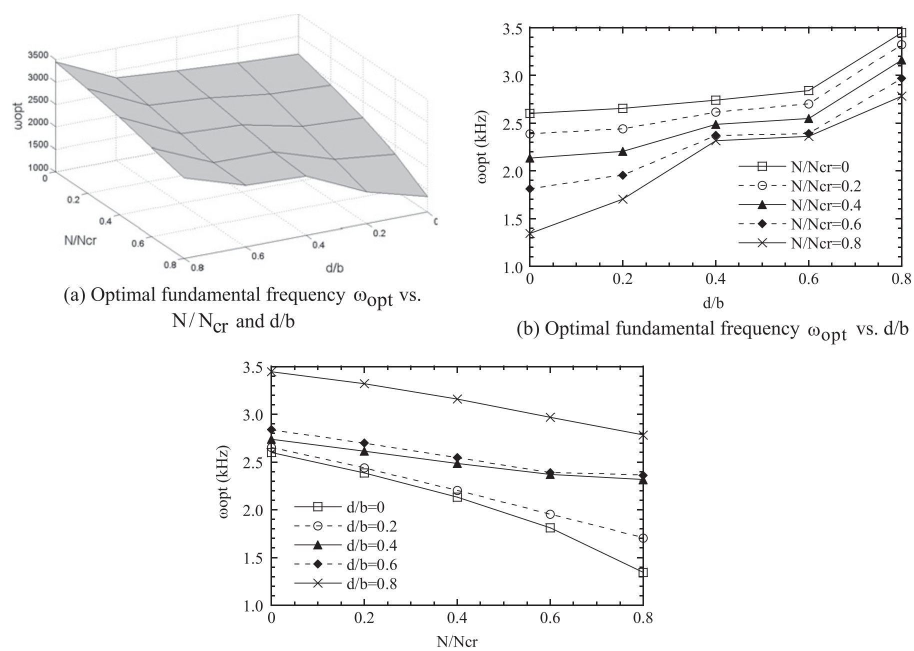

(a) Optimal fundamental frequency ω_{opt} vs. N/N_{cr} and d/b

(b) Optimal fundamental frequency ω_{opt} vs. d/b

(c) Optimal fundamental frequency ω_{opt} vs. N/N_{cr}

Fig. 8. Effect of cutout size and in-plane compressive force on optimal fundamental frequency of $[\pm\theta/90/0]_{2s}$ simply supported laminated curved panels with central circular cutout (b = 10 cm, a/b = 1, ϕ = 60°).

compressive forces N are considered (Fig. 3). The simply supported boundary condition prevents out of plane displacement w, but allows in-plane movements u and v. The meshes selected for the finite element analysis are based on the convergent studies performed by the author [32] and no symmetry simplifications are made for those laminated curved panels. In the analyses, the width b of the curved panel is equal to 10 cm. The cutout size d varies from 0 to 8 cm. The circular angle ϕ varies from 5° to 120°. To study the influence of axial compressive force on the results of optimization, N = 0, 0.2N_{cr}, 0.4N_{cr}, 0.6N_{cr}, and 0.8N_{cr}, are selected, where N_{cr} is the linearized critical buckling loads of the laminated curved panels.

The lamina of the curved panels consists of Graphite/Epoxy and material constitutive properties are taken from Crawley [1], which are E_{11} = 128 GPa, E_{22} = 11 GPa, G_{23} = 1.53 GPa, $G_{12} = G_{13}$ = 4.48 GPa, ν_{12} = 0.25, and ρ = 1500 kg/m^3. The thickness of each ply is 0.125 mm and the laminate layup of the laminated curved panel is $[\pm\theta/90/0]_{2s}$.

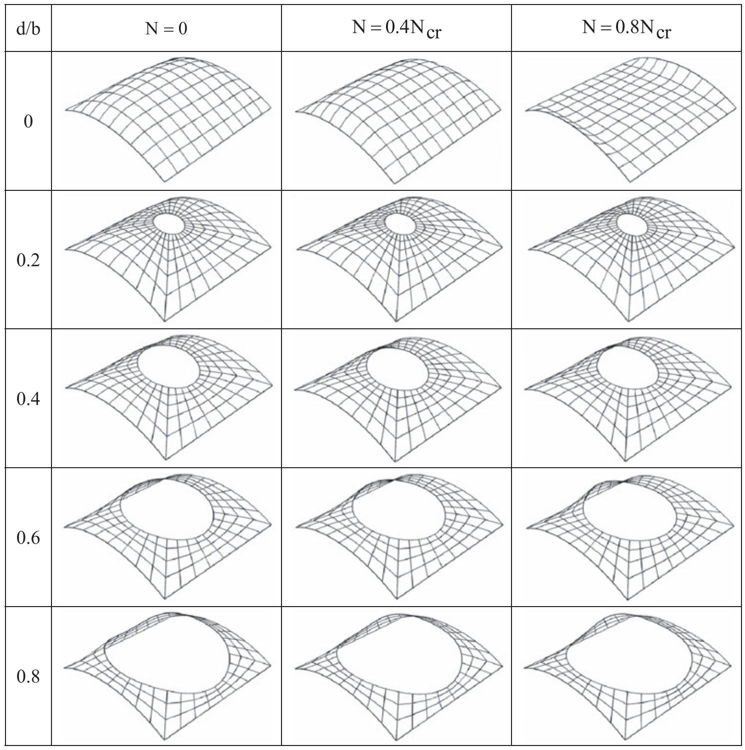

Fig. 9. Fundamental vibration modes of $[\pm\theta/90/0]_{2s}$ simply supported laminated curved panels with central circular cutout and under optimal fiber angles (b = 10 cm, a/b = 1, ϕ = 60°).

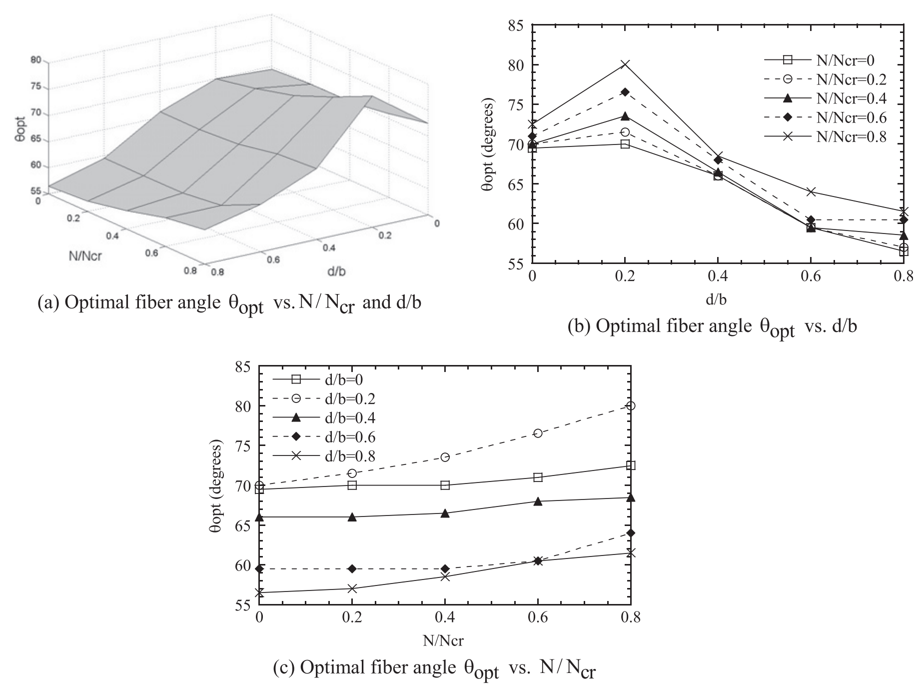

Fig. 10. Effect of cutout size and in-plane compressive force on optimal fiber angle of $[\pm\theta/90/0]_{2s}$ simply supported laminated curved panels with central circular cutout (b = 10 cm, a/b = 1, ϕ = 120°).

5.1. Laminated curved panels with aspect ratio a/b = 1

5.1.1. Panels with circular angle ϕ = 5°

In this section, the aspect ratio a/b of the laminated curved panels is equal to 1 and the circular angle ϕ is equal to 5°. To find the optimal fiber angle θ and the associated optimal fundamental frequency ω of each laminated curved panel, we can express the optimization problem as:

$$\text{Maximize}: \omega(\theta) \tag{13a}$$

$$\text{Subjected to}: 0^\circ \leqslant \theta \leqslant 90^\circ \tag{13b}$$

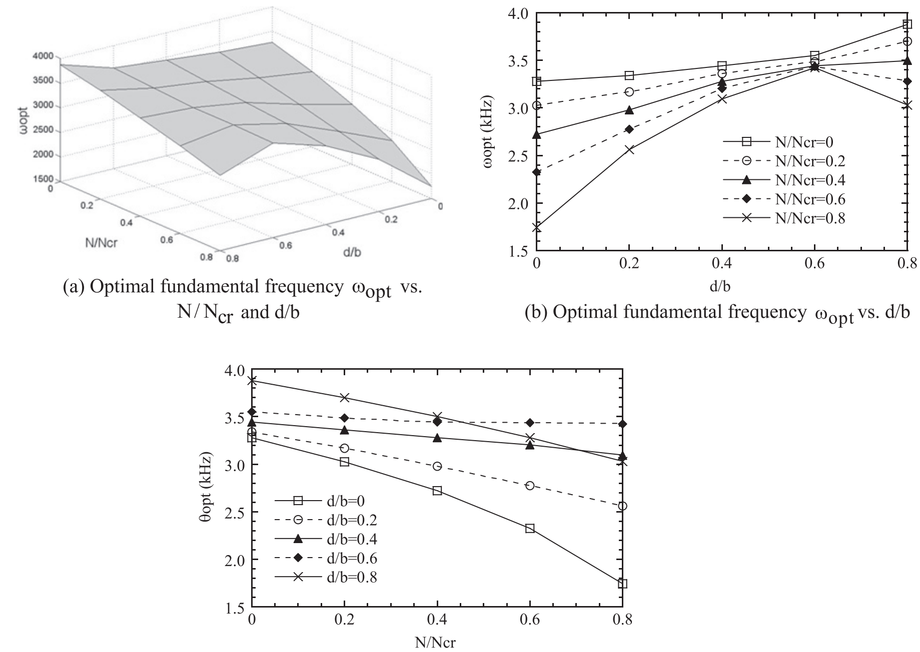

(a) Optimal fundamental frequency ω_{opt} vs. N/N_{cr} and d/b

(b) Optimal fundamental frequency ω_{opt} vs. d/b

(c) Optimal fundamental frequency ω_{opt} vs. N/N_{cr}

Fig. 11. Effect of cutout size and in-plane compressive force on optimal fundamental frequency of $[\pm\theta/90/0]_{2s}$ simply supported laminated curved panels with central circular cutout (b = 10 cm, a/b = 1, ϕ = 120°).

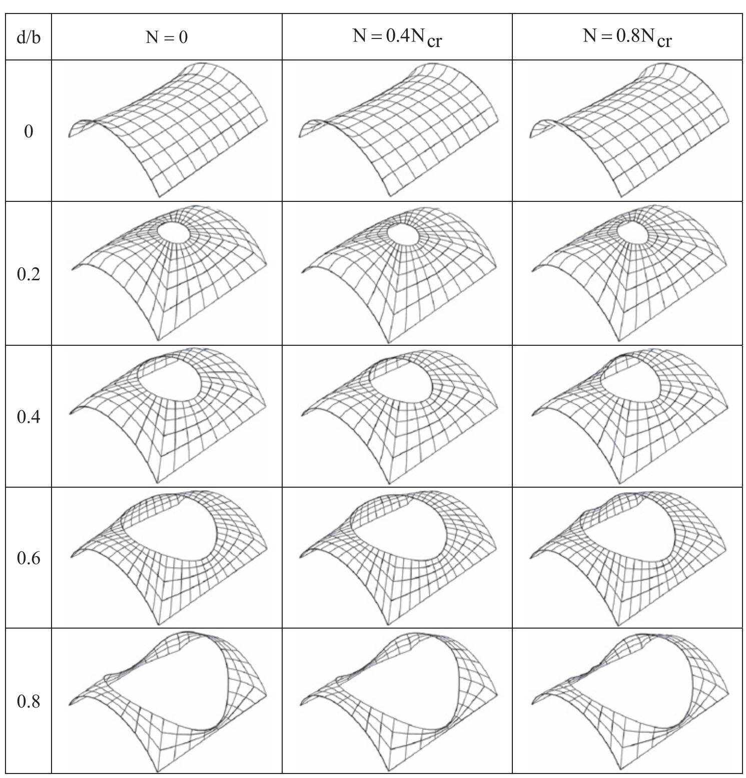

Fig. 12. Fundamental vibration modes of $[\pm\theta/90/0]_{2s}$ simply supported laminated curved panels with central circular cutout and under optimal fiber angles (b = 10 cm, a/b = 1, ϕ = 120°).

Before the golden section method is carried out, the fundamental frequency ω of the laminated curved panel is calculated by employing the Abaqus finite element program for every 10° increment in θ angle to locate the maximum point approximately. Then proper upper and lower bounds are selected and the golden section method is performed. The optimization process is terminated when an absolute tolerance (the difference of the two intermediate points between the upper bound and the lower bound) $\Delta\theta \leqslant 0.5°$ is reached.

Fig. 4a shows a three dimensional plot of the optimal fiber angle θ_{opt} versus d/b and N/N_{cr} for $[\pm\theta/90/0]_{2s}$ laminated curved panel

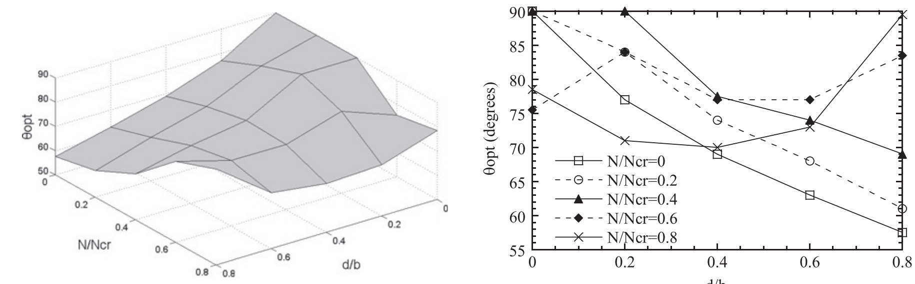

(a) Optimal fiber angle θ_{opt} vs. N/N_{cr} and d/b

(b) Optimal fiber angle θ_{opt} vs. d/b

(c) Optimal fiber angle θ_{opt} vs. N/N_{cr}

Fig. 13. Effect of cutout size and in-plane compressive force on optimal fiber angle of $[\pm\theta/90/0]_{2s}$ simply supported laminated curved panels with central circular cutout (b = 10 cm, a/b = 2, ϕ = 5°).

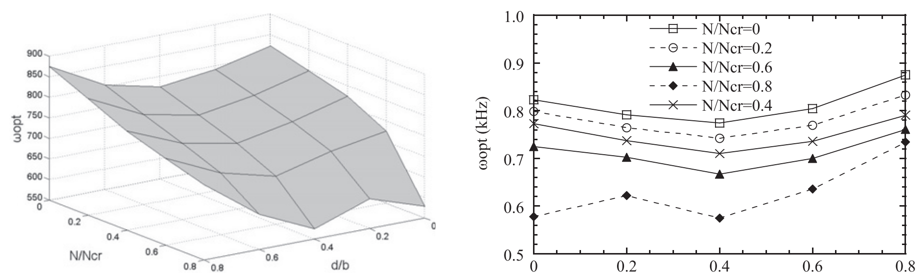

(a) Optimal fundamental frequency ω_{opt} vs. N/N_{cr} and d/b

(b) Optimal fundamental frequency ω_{opt} vs. d/b

(c) Optimal fundamental frequency ω_{opt} vs. N/N_{cr}

Fig. 14. Effect of cutout size and in-plane compressive force on optimal fundamental frequency of $[\pm\theta/90/0]_{2s}$ simply supported laminated curved panels with central circular cutout (b = 10 cm, a/b = 2, ϕ = 5°).

with aspect ratio a/b = 1 and ϕ = 5°. Fig. 4b and Fig. 4c show the same plot as Fig. 4a, but projected into two dimensional planes with different viewpoints. From these figures, we can see that the optimal fiber angles are very close to 45° for all the panels and seem not sensitive to the cutout size and axial compressive force.

Fig. 5a shows the associated optimal fundamental frequency ω_{opt} versus d/b and N/N_{cr}. Again, Fig. 5b and Fig. 5c show the same plot as Fig. 5a, but projected into two dimensional planes. From these figures, we can see that the optimal fundamental frequency increases with the increasing of the cutout size. This is because a panel with a large cutout is more like four stubby panels. As a consequence, one could expect frequencies to increase with d/b ratio. This phenomenon has also been found by other investigators [6,8–12]. In addition, we can observe that the optimal fundamental frequency decreases with the increasing of the axial compressive force.

Fig. 6 shows the fundamental vibration modes of the typical laminated curved panels under optimal fiber angle conditions. It

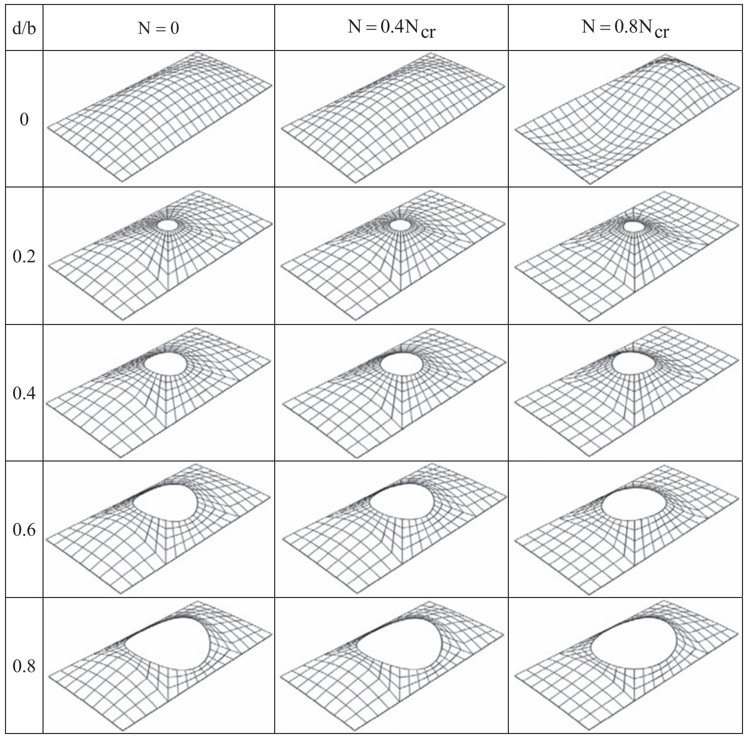

Fig. 15. Fundamental vibration modes of $[\pm\theta/90/0]_{2s}$ simply supported laminated curved panels with central circular cutout and under optimal fiber angles (b = 10 cm, a/b = 2, ϕ = 5°).

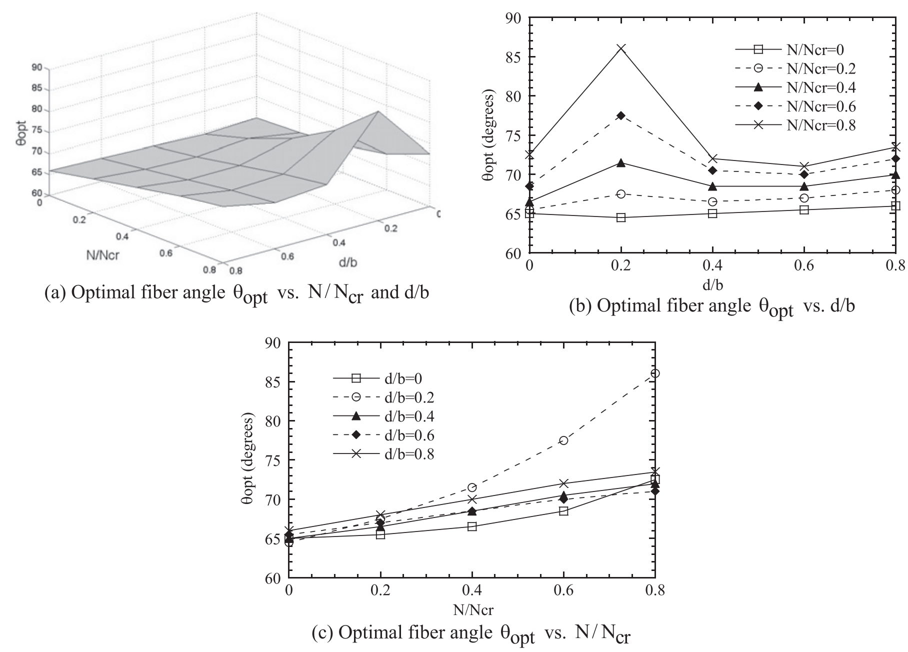

Fig. 16. Effect of cutout size and in-plane compressive force on optimal fiber angle of $[\pm\theta/90/0]_{2s}$ simply supported laminated curved panels with central circular cutout (b = 10 cm, a/b = 2, ϕ = 60°).

can be seen that all panels vibrate into a half sine wave in both longitudinal and circumferential directions.

5.1.2. Panels with circular angle ϕ = 60°

In this section, the aspect ratio a/b of the laminated curved panels is still equal to 1 but the circular angle ϕ is changed to 60°. Fig. 7 shows the influence of the cut size and axial compressive force on the optimal fiber angle of these panels. Comparing Fig. 7 with Fig. 4, we can observe that when the curvatures of these panels are increased, the optimal fiber angles are significantly influenced by the cutout size and axial compressive force.

Fig. 8 shows the influence of the cut size and axial compressive force on the optimal fundamental frequency of these panels. It shows the similar trend as Fig. 5, i.e. the optimal fundamental frequency increases with the increasing of the cutout size and decreases with the increasing of the axial compressive force.

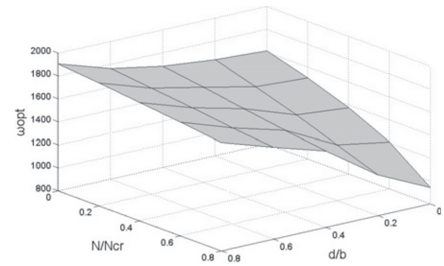

(a) Optimal fundamental frequency ω_{opt} vs. N/N_{cr} and d/b

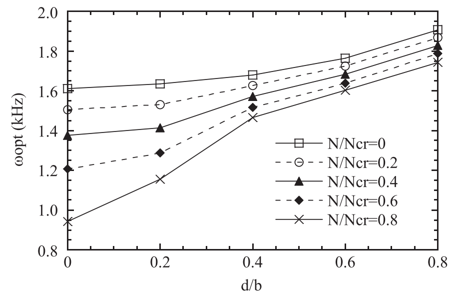

(b) Optimal fundamental frequency ω_{opt} vs. d/b

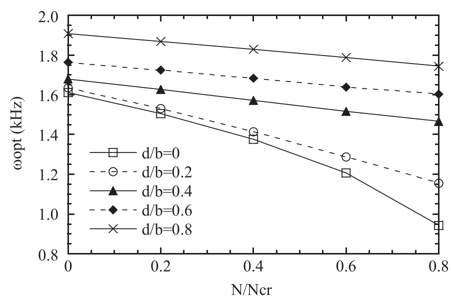

(c) Optimal fundamental frequency ω_{opt} vs. N/N_{cr}

Fig. 17. Effect of cutout size and in-plane compressive force on optimal fundamental frequency of $[\pm\theta/90/0]_{2s}$ simply supported laminated curved panels with central circular cutout (b = 10 cm, a/b = 2, ϕ = 60°).

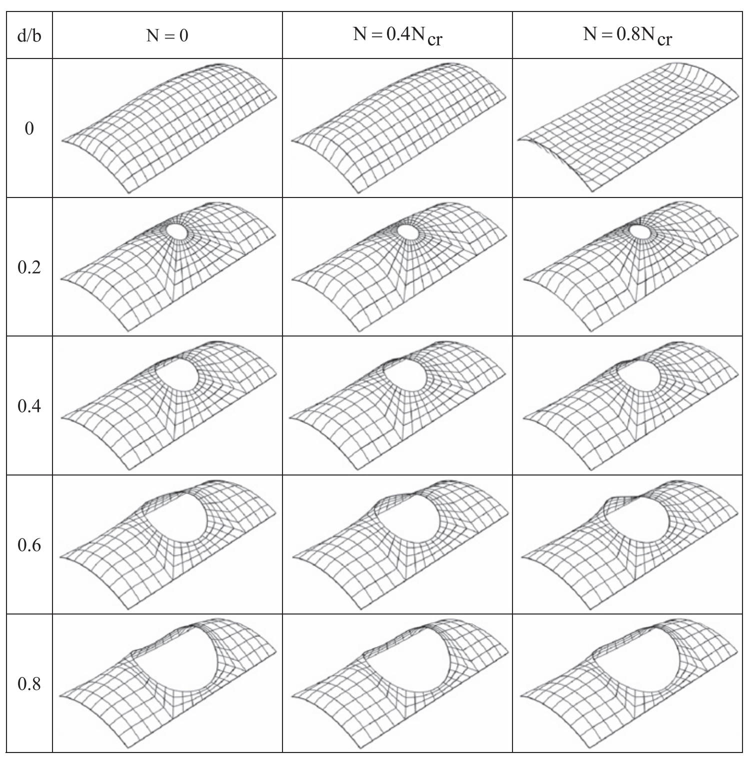

Fig. 18. Fundamental vibration modes of $[\pm\theta/90/0]_{2s}$ simply supported laminated curved panels with central circular cutout and under optimal fiber angles (b = 10 cm, a/b = 2, ϕ = 60°).

However, we can notice that the optimal fundamental frequencies of laminated curved panels with large curvatures (Fig. 8) are higher than those with small curvatures (Fig. 5).

Fig. 9 shows the fundamental vibration modes of the typical laminated curved panels under optimal fiber angle condition. Again, all panels vibrate into a half sine wave in both longitudinal and circumferential directions.

5.1.3. Panels with circular angle ϕ = 120°

In this section, the aspect ratio a/b of the laminated curved panels is still equal to 1 but the circular angle ϕ is changed to 120°. Fig. 10 shows the influence of the cut size and axial compressive force on the optimal fiber angle of these panels. Comparing Fig. 10 with Figs. 7 and 4, we can conclude that when the curvatures of laminated curved panels are large, the optimal fiber angles

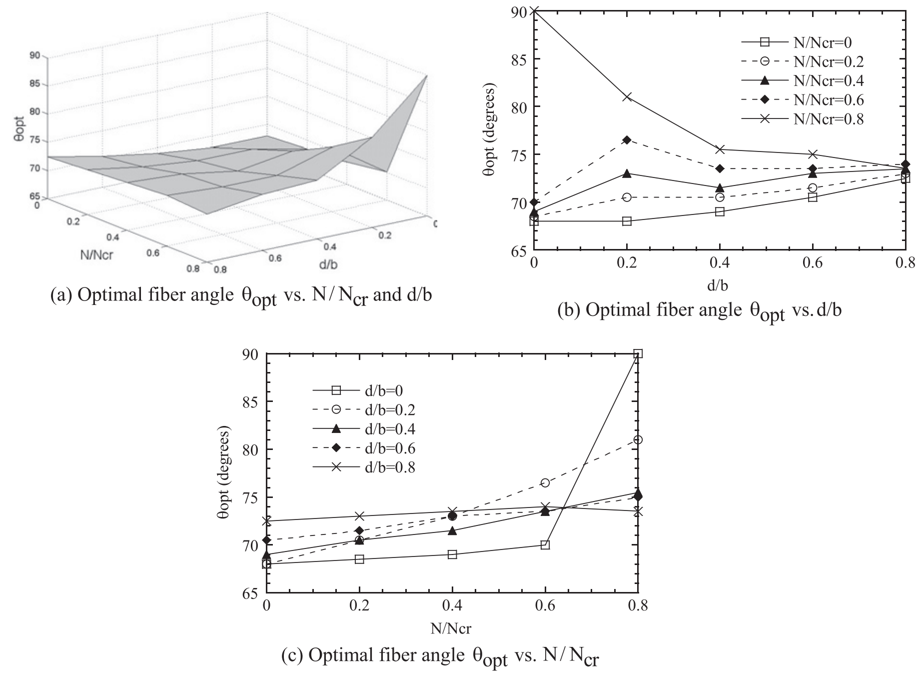

Fig. 19. Effect of cutout size and in-plane compressive force on optimal fiber angle of $[\pm\theta/90/0]_{2s}$ simply supported laminated curved panels with central circular cutout (b = 10 cm, a/b = 2, ϕ = 120°).

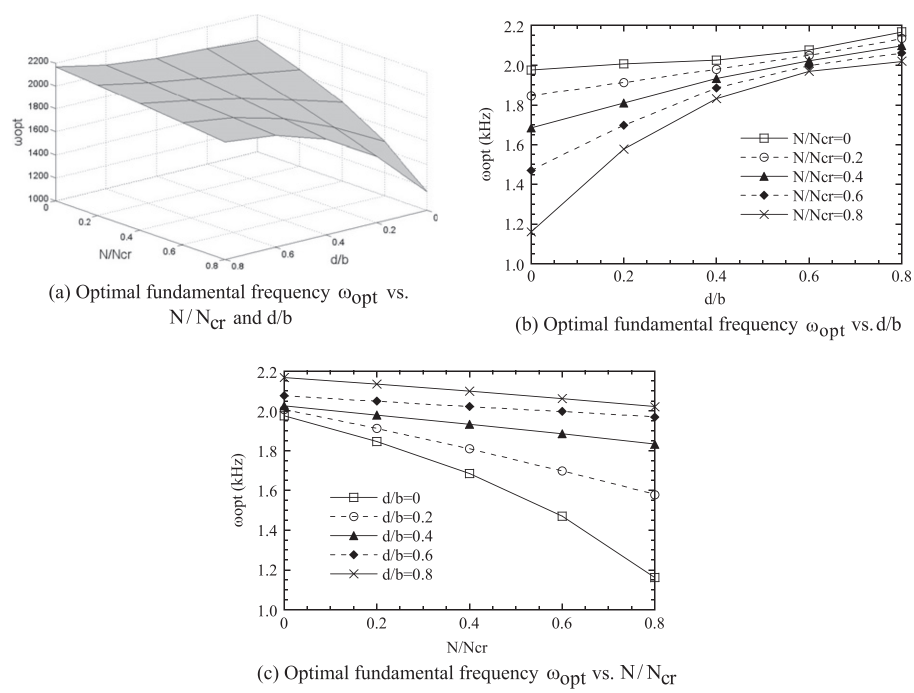

Fig. 20. Effect of cutout size and in-plane compressive force on optimal fundamental frequency of $[\pm\theta/90/0]_{2s}$ simply supported laminated curved panels with central circular cutout (b = 10 cm, a/b = 2, ϕ = 120°).

are significantly influenced by the cutout size and axial compressive force.

Fig. 11 shows the influence of the cut size and axial compressive force on the optimal fundamental frequency of these panels. Comparing Fig. 11 with Figs. 8 and 5, we can conclude that the optimal fundamental frequency usually increases with the increasing of the cutout size and decreases with the increasing of the axial compressive force. Also, the optimal fundamental frequencies of laminated curved panels with large curvatures are higher than those with small curvatures.

Fig. 12 shows the fundamental vibration modes of the typical laminated curved panels under optimal fiber angle condition. Again, all panels vibrate into a half sine wave in both longitudinal and circumferential directions.

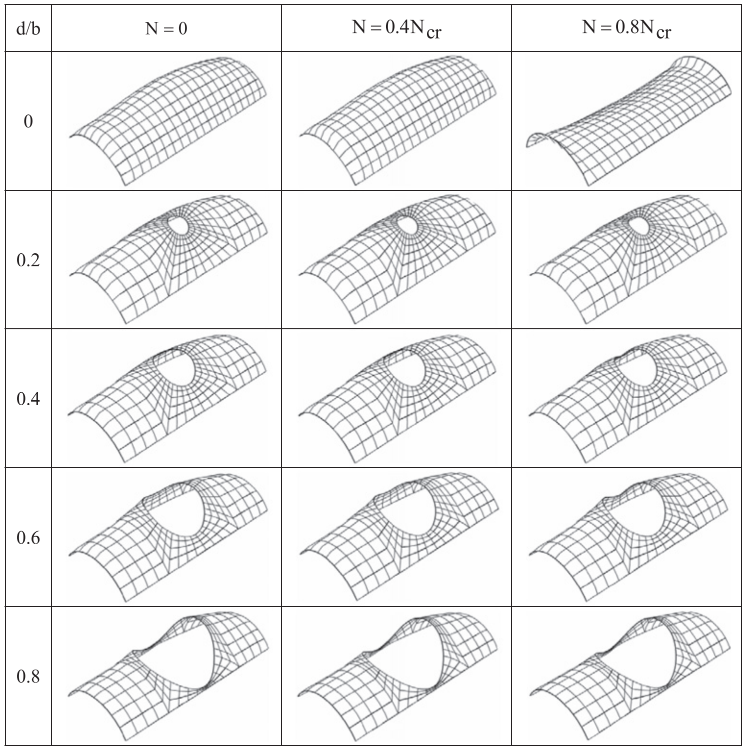

Fig. 21. Fundamental vibration modes of $[\pm\theta/90/0]_{2s}$ simply supported laminated curved panels with central circular cutout and under optimal fiber angles (b = 10 cm, a/b = 2, ϕ = 120°).

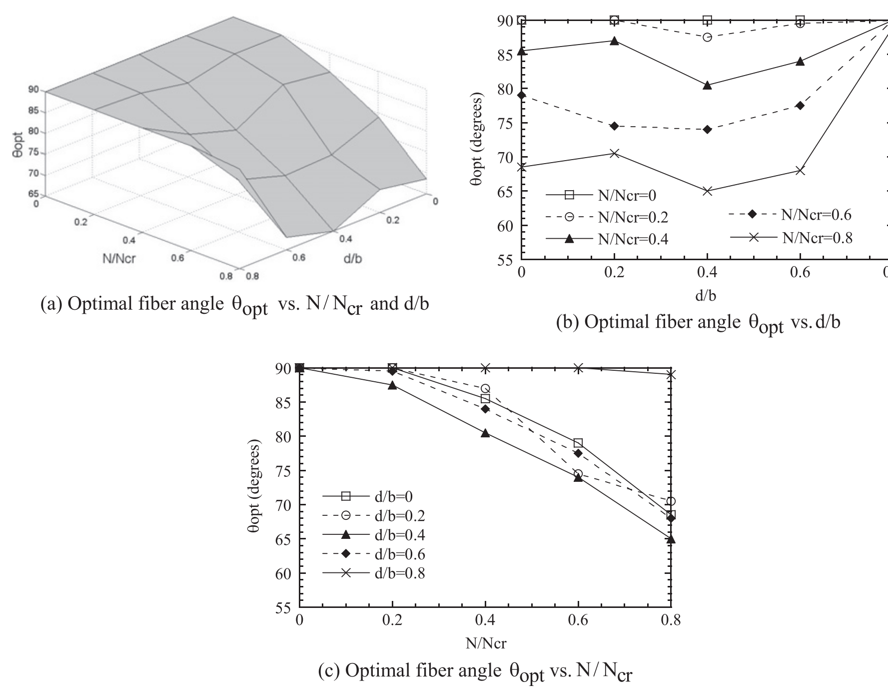

Fig. 22. Effect of cutout size and in-plane compressive force on optimal fiber angle of $[\pm\theta/90/0]_{2s}$ simply supported laminated curved panels with central circular cutout (b = 10 cm, a/b = 3, ϕ = 5°).

5.2. Laminated curved panels with aspect ratio a/b = 2

5.2.1. Panels with circular angle ϕ = 5°

In this section, the laminated curved panels with aspect ratio a/b = 2 and circular angle ϕ = 5° are analyzed. Fig. 13 shows the influence of the cut size and axial compressive force on the optimal fiber angle of these panels. Comparing Fig. 13 with Fig. 4, we can observe that when the aspect ratios of these panels are increased, the optimal fiber angles are significantly influenced by the cutout size and axial compressive force.

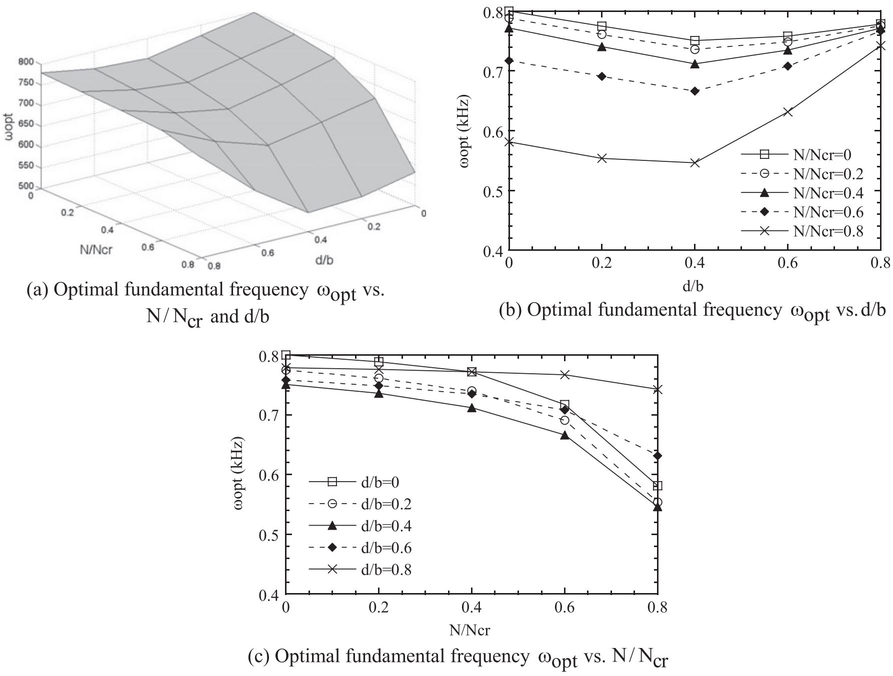

(a) Optimal fundamental frequency ω_{opt} vs. N/N_{cr} and d/b

(b) Optimal fundamental frequency ω_{opt} vs. d/b

(c) Optimal fundamental frequency ω_{opt} vs. N/N_{cr}

Fig. 23. Effect of cutout size and in-plane compressive force on optimal fundamental frequency of $[\pm\theta/90/0]_{2s}$ simply supported laminated curved panels with central circular cutout (b = 10 cm, a/b = 3, ϕ = 5°).

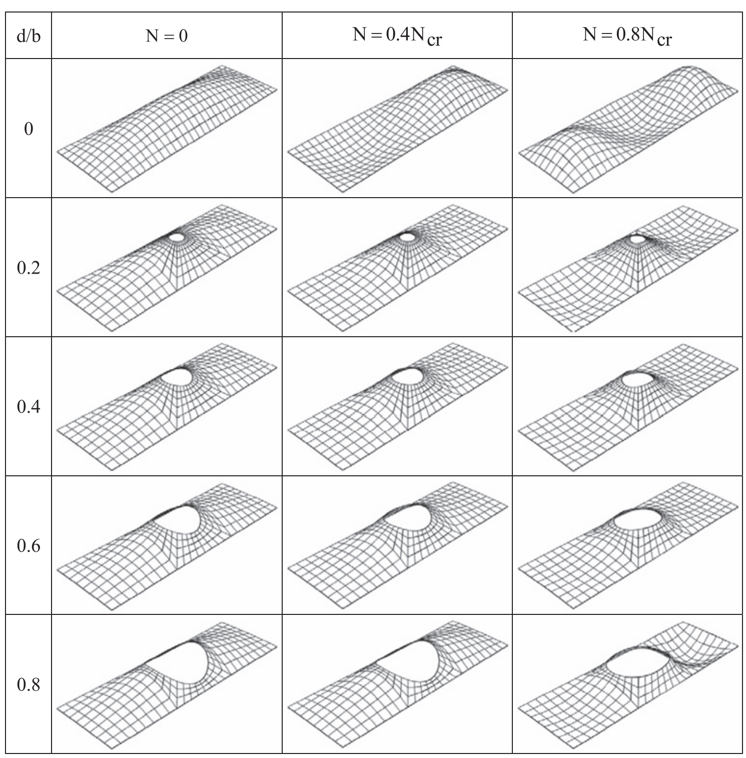

Fig. 24. Fundamental vibration modes of $[\pm\theta/90/0]_{2s}$ simply supported laminated curved panels with central circular cutout and under optimal fiber angles (b = 10 cm, a/b = 3, ϕ = 5°).

Fig. 14 shows the influence of the cut size and axial compressive force on the optimal fundamental frequency of these panels. It shows that the optimal fundamental frequency initially decreases with the increasing of the cutout size. However, after a certain size of cutout has been reached, the optimal fundamental frequency starts to increases with the increasing of the cutout size. On the other hand, the optimal fundamental frequency still decreases with the increasing of the axial compressive force. Comparing Fig. 14 with Fig. 5, we can observe that the optimal fundamental frequencies of laminated curved panels with large

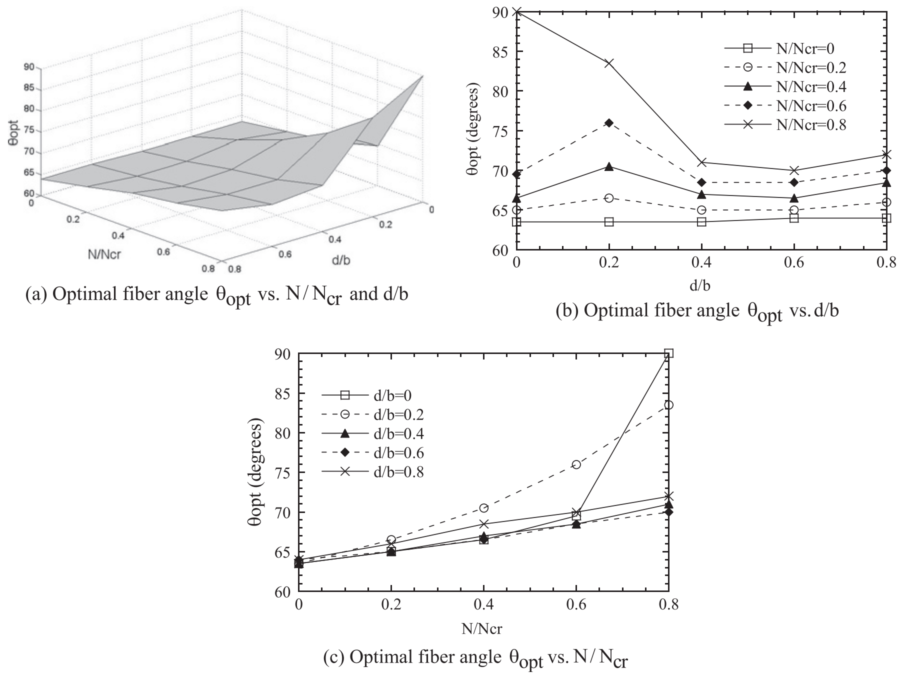

Fig. 25. Effect of cutout size and in-plane compressive force on optimal fiber angle of $[\pm\theta/90/0]_{2s}$ simply supported laminated curved panels with central circular cutout (b = 10 cm, a/b = 3, ϕ = 60°).

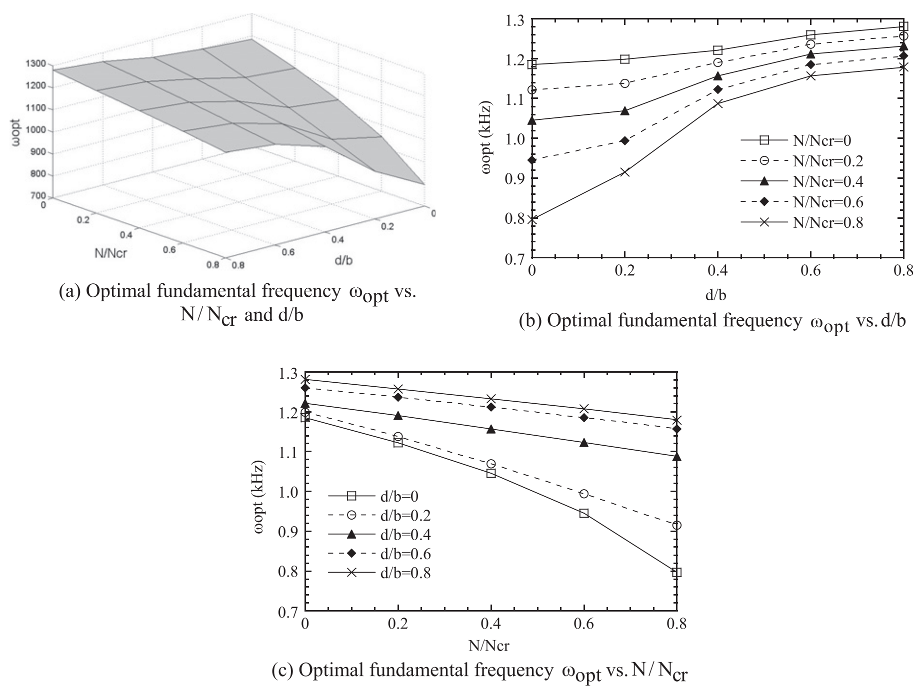

Fig. 26. Effect of cutout size and in-plane compressive force on optimal fundamental frequency of $[\pm\theta/90/0]_{2s}$ simply supported laminated curved panels with central circular cutout (b = 10 cm, a/b = 3, ϕ = 60°).

aspect ratios (Fig. 14) are lower than those with small curvatures (Fig. 5).

Fig. 15 shows the fundamental vibration modes of the typical laminated curved panels under optimal fiber angle condition. It can be seen that most of the panels vibrate into a half sine wave in both longitudinal and circumferential directions. However, for panel with no cutout and subjected to high compressive force (say $N = 0.8N_{cr}$), its vibration mode may have two half sine waves in the longitudinal direction.

5.2.2. Panels with circular angle ϕ = 60°

In this section, the laminated curved panels with aspect ratio a/b = 2 and circular angle ϕ = 60° are analyzed. Fig. 16 shows the influence of the cut size and axial compressive force on the optimal

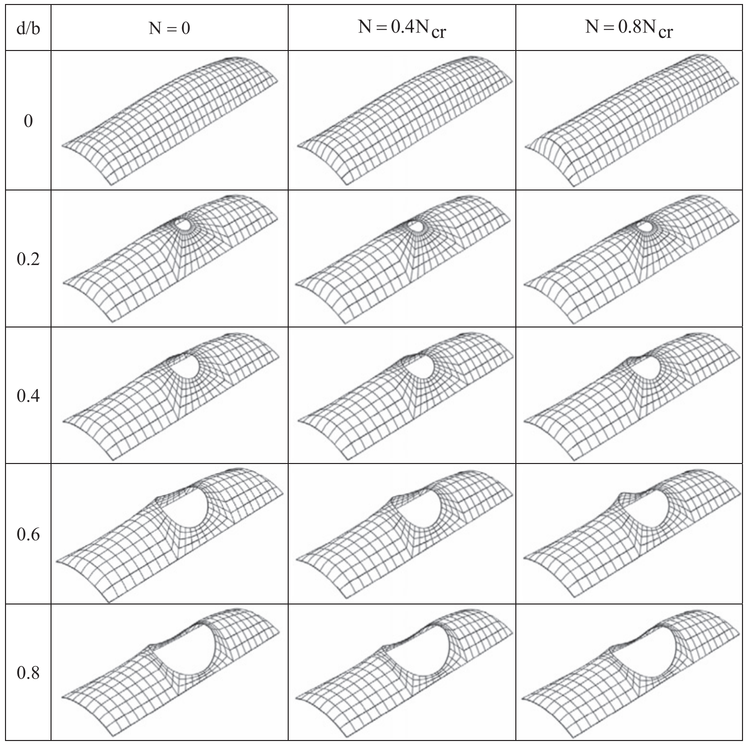

Fig. 27. Fundamental vibration modes of $[\pm\theta/90/0]_{2S}$ simply supported laminated curved panels with central circular cutout and under optimal fiber angles (b = 10 cm, a/b = 3, ϕ = 60°).

fiber angle of these panels. Comparing Fig. 16 with Figs. 13 and 7, we can observe that the optimal fiber angles are significantly influenced by the cutout size, axial compressive force, curvature and aspect ratio of the laminated curved panels.

Fig. 17 shows the influence of the cut size and axial compressive force on the optimal fundamental frequency of these panels. It shows that the optimal fundamental frequency increases with the increasing of the cutout size and decreases with the increasing of the axial compressive force. Comparing Fig. 17 with Fig. 8, we can confirm that the optimal fundamental frequencies of laminated curved panels with large aspect ratios are lower than those with small aspect ratio. Comparing Fig. 17 with Fig. 14, we can confirm that the optimal fundamental frequencies of laminated curved panels with large curvatures are higher than those with small curvatures.

Fig. 18 shows the fundamental vibration modes of the typical laminated curved panels under optimal fiber angle condition. It can be seen that all of the panels vibrate into a half sine wave in both longitudinal and circumferential directions.

5.2.3. Panels with circular angle ϕ = 120°

In this section, the laminated curved panels with aspect ratio a/b = 2 and circular angle ϕ = 120° are analyzed. Fig. 19 shows the influence of the cut size and axial compressive force on the optimal fiber angle of these panels. Comparing Fig. 19 with Figs. 16, 13 and 10, we can observe again that the optimal fiber angles are significantly influenced by the cutout size, axial compressive force, curvature and aspect ratio of the laminated curved panels.

Fig. 20 shows the influence of the cut size and axial compressive force on the optimal fundamental frequency of these panels. It shows the similar trend as before. Comparing Fig. 20 with Fig. 11, we can reconfirm that the optimal fundamental frequencies of laminated curved panels with large aspect ratios are lower than those with small aspect ratio. Comparing Fig. 20 with Figs. 17 and 14, we can reconfirm that the optimal fundamental frequencies of laminated curved panels with large curvatures are higher than those with small curvatures.

Fig. 21 shows the fundamental vibration modes of the typical laminated curved panels under optimal fiber angle condition. It can be seen that all of the panels vibrate into a half sine wave in both longitudinal and circumferential directions.

5.3. Laminated curved panels with aspect ratio a/b = 3

5.3.1. Panels with circular angle ϕ = 5°

In this section, the laminated curved panels with aspect ratio a/b = 3 and circular angle ϕ = 5° are analyzed. Fig. 22 shows the influence of the cut size and axial compressive force on the optimal fiber angle of these panels. Comparing Fig. 22 with Figs. 13 and 4, we can observe again that when the aspect ratios of these panels are increased, the optimal fiber angles are significantly influenced by the cutout size and axial compressive force.

Fig. 23 shows the influence of the cut size and axial compressive force on the optimal fundamental frequency of these panels. It shows similar trend as Fig. 14. The optimal fundamental frequency initially decreases with the increasing of the cutout size. However, after a certain size of cutout has been reached, the optimal fundamental frequency starts to increases with the increasing of the cutout size. On the other hand, the optimal fundamental frequency still decreases with the increasing of the axial compressive force. Comparing Fig. 23 with Figs. 14 and 5, we can conclude that the optimal fundamental frequencies of laminated curved panels with large aspect ratios are lower than those with small curvatures.

Fig. 24 shows the fundamental vibration modes of the typical laminated curved panels under optimal fiber angle condition. It can be seen that most of the panels vibrate into a half sine wave in both longitudinal and circumferential directions. However, for panels with or without cutout and subjected to high compressive force (say $N = 0.8N_{cr}$), their vibration modes may have three half sine waves in the longitudinal direction.

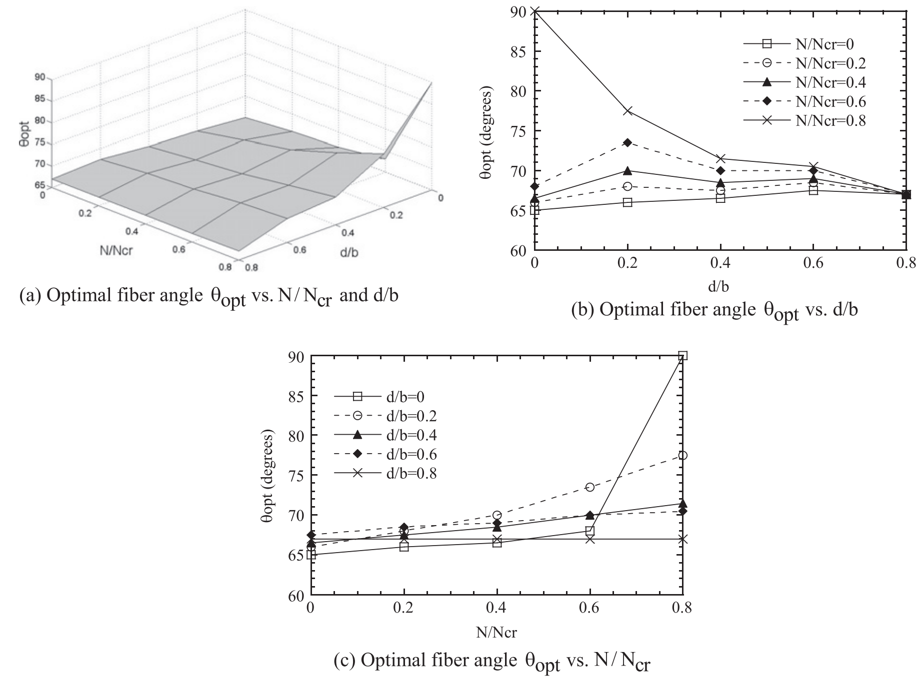

(a) Optimal fiber angle θ_{opt} vs. N/N_{cr} and d/b

(b) Optimal fiber angle θ_{opt} vs. d/b

(c) Optimal fiber angle θ_{opt} vs. N/N_{cr}

Fig. 28. Effect of cutout size and in-plane compressive force on optimal fiber angle of $[\pm\theta/90/0]_{2s}$ simply supported laminated curved panels with central circular cutout (b = 10 cm, a/b = 3, ϕ = 120°).

5.3.2. Panels with circular angle ϕ = 60°

In this section, the laminated curved panels with aspect ratio a/b = 3 and circular angle ϕ = 60° are analyzed. Fig. 25 shows the influence of the cut size and axial compressive force on the optimal fiber angle of these panels. Comparing Fig. 25 with Figs. 16, 7 and 22, we can observe that the optimal fiber angles are significantly influenced by the cutout size, axial compressive force, curvature and aspect ratio of the laminated curved panels.

Fig. 26 shows the influence of the cut size and axial compressive force on the optimal fundamental frequency of these panels. It shows that the optimal fundamental frequency increases with the increasing of the cutout size and decreases with the increasing of the axial compressive force. Comparing Fig. 26 with Figs. 17 and 8, we can confirm that the optimal fundamental frequencies of laminated curved panels with large aspect ratios are lower than those with small aspect ratio. Comparing Fig. 26 with Fig. 23, we

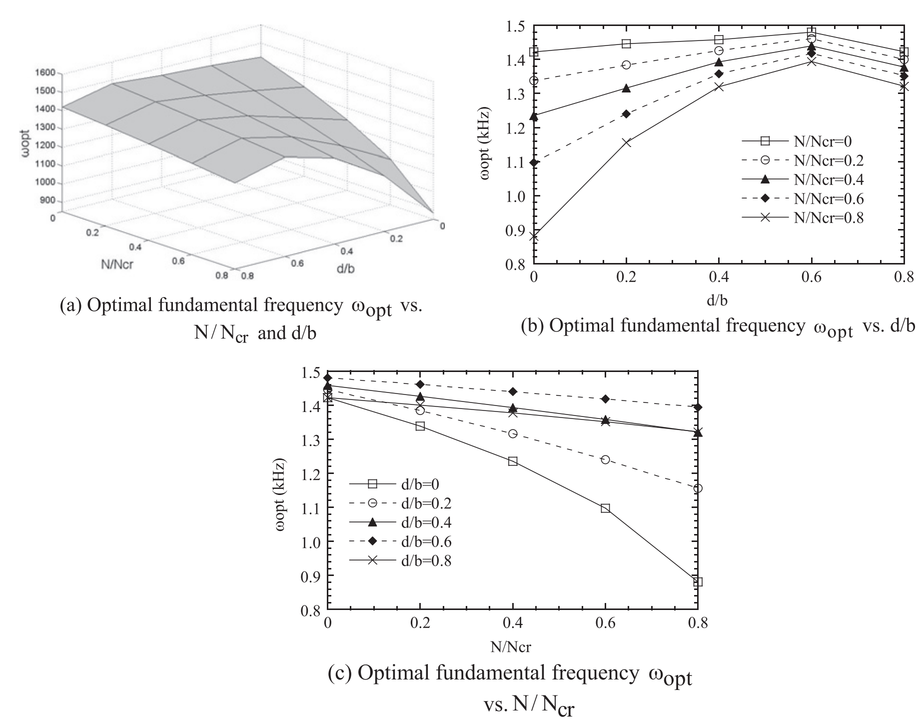

(a) Optimal fundamental frequency ω_{opt} vs. N/N_{cr} and d/b

(b) Optimal fundamental frequency ω_{opt} vs. d/b

(c) Optimal fundamental frequency ω_{opt} vs. N/N_{cr}

Fig. 29. Effect of cutout size and in-plane compressive force on optimal fundamental frequency of $[\pm\theta/90/0]_{2s}$ simply supported laminated curved panels with central circular cutout (b = 10 cm, a/b = 3, ϕ = 120°).

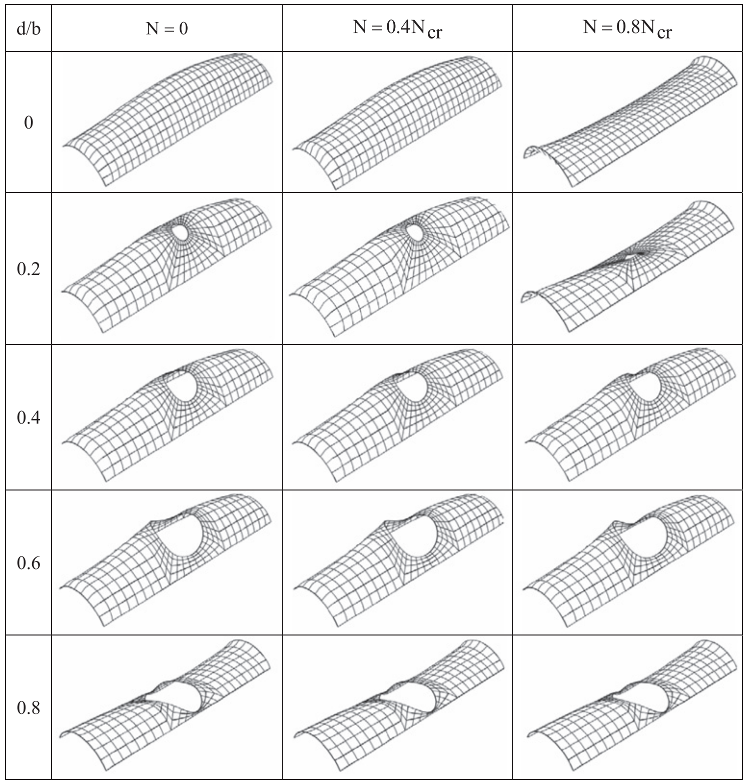

Fig. 30. Fundamental vibration modes of $[\pm\theta/90/0]_{2s}$ simply supported laminated curved panels with central circular cutout and under optimal fiber angles (b = 10 cm, a/b = 3, ϕ = 120°).

can confirm that the optimal fundamental frequencies of laminated curved panels with large curvatures are higher than those with small curvatures.

Fig. 27 shows the fundamental vibration modes of the typical laminated curved panels under optimal fiber angle condition. It can be seen that all of the panels vibrate into a half sine wave in both longitudinal and circumferential directions.

5.3.3. Panels with circular angle ϕ = 120°

In this section, the laminated curved panels with aspect ratio $a/b = 3$ and circular angle $\phi = 120°$ are analyzed. Fig. 28 shows the influence of the cut size and axial compressive force on the optimal fiber angle of these panels. Comparing Fig. 28 with Figs. 25, 22, 19 and 10, we can conclude that the optimal fiber angles are significantly influenced by the cutout size, axial compressive force, curvature and aspect ratio of the laminated curved panels.

Fig. 29 shows the influence of the cut size and axial compressive force on the optimal fundamental frequency of these panels. It shows the similar trend as before. Comparing Fig. 29 with Fig. 20 and 11, we can conclude that the optimal fundamental frequencies of laminated curved panels with large aspect ratios are lower than those with small aspect ratio. Comparing Fig. 29 with Figs. 26 and 23, we can conclude that the optimal fundamental frequencies of laminated curved panels with large curvatures are higher than those with small curvatures.

Fig. 30 shows the fundamental vibration modes of the typical laminated curved panels under optimal fiber angle condition. It can be seen that all of the panels vibrate into a half sine wave in both longitudinal and circumferential directions.

6. Conclusions

Based on the numerical results of this investigation, the following specific conclusions may be drawn:

1. The optimal fiber angles of laminated curved panels are significantly influenced by the cutout size, axial compressive force, curvature and aspect ratio. However, for laminated curved panels with small aspect ratio (say $a/b = 1$) and small curvature (say $\phi = 5°$), the optimal fiber angles are not sensitive to the cutout size and axial compressive force.
2. The optimal fundamental frequency of laminated curved panels usually increases with the increasing of the cutout size. However, for laminated curved panels with large aspect ratio (say $a/b \geqslant 2$) and small curvature (say $\phi = 5°$), the optimal fundamental frequency initially decreases with the increasing of the cutout size. After a certain size of cutout has been reached, the optimal fundamental frequency starts to increases with the increasing of the cutout size.
3. The optimal fundamental frequency of laminated curved panels decreases with the increasing of the axial compressive force.
4. The optimal fundamental frequencies of laminated curved panels with large aspect ratios are lower than those with small aspect ratios.
5. The optimal fundamental frequencies of laminated curved panels with large curvatures are higher than those with small curvatures.
6. Under the optimal fiber angle conditions, the laminated curved panels with or without cutouts usually vibrate into a half sine wave in both longitudinal and circumferential directions. However, for panels with small curvature (say $\phi = 5°$), large aspect ratio (say $a/b \geqslant 2$) and subjected to high compressive force (say $N = 0.8N_{cr}$), their vibration modes may have more half sine waves in the longitudinal direction.

This study investigates the influences of the panel aspect ratio, the panel curvature, the cutout size and the compressive force on the maximum fundamental natural frequencies, the optimal fiber orientations and the associated fundamental vibration modes of the laminated curved panels with $[\pm\theta/90/0]_{2s}$ laminated layup. All the results are presented by the dimensionless quantities, such as a/b, d/b and N/N_{cr}. Thus, they can be applicable to the panels with other sizes and different initial stress levels but limited to the lamination $[\pm\theta/90/0]_{2s}$.

Acknowledgment

This research work was financially supported by the National Science Council of the Republic of China under Grant NSC 101-2221-E-006-238.

References

[1] Crawley EF. The natural modes of graphite/epoxy cantilever plates and shells. J Compos Mater 1979;13(3):195–205.
[2] Chandrashekhara K. Free vibration of anisotropic laminated doubly curved shells. Comput Struct 1989;33(2):435–40.
[3] Qatu MS, Leissa AW. Natural frequencies for cantilevered doubly-curved laminated composite shallow shells. Compos Struct 1991;17(3):227–55.
[4] Raouf RA. Tailoring the dynamic characteristics of composite panels using fiber orientation. Compos Struct 1994;29(3):259–67.
[5] Chun L, Lam KY. Dynamic analysis of clamped laminated curved panels. Compos Struct 1995;30(4):389–98.
[6] Hu H-T, Juang C-D. Maximization of the fundamental frequencies of laminated curved panels against fiber orientation. J Aircraft, AIAA 1997;34(6):792–801.
[7] Hu H-T, Tsai J-Y. Maximization of the fundamental frequencies of laminated cylindrical shells with respect to fiber orientations. J Sound Vib 1999;225(4):723–40.
[8] Hu H-T, Ou S-C. Maximization of the fundamental frequencies of laminated truncated conical shells with respect to fiber orientations. Compos Struct 2001;52(3–4):265–75.
[9] Hu H-T, Tsai W-K. Maximization of the fundamental frequencies of axially compressed laminated plates against fiber orientation. AIAA J 2009;27(4):916–22.
[10] Lee HP, Lim SP, Chow ST. Free vibration of composite rectangular plates with rectangular cutouts. Compos Struct 1987;8(1):63–81.
[11] Ramakrishna S, Rao KM, Rao NS. Free vibration analysis of laminates with circular cutout by hybrid-stress finite element. Compos Struct 1992;21(3):177–85.
[12] Hu H-T, Ho M-H. Influence of geometry and end conditions on optimal fundamental natural frequencies of symmetrically laminated plates. J Reinf Plast Compos 1996;15(9):877–93.
[13] Sivakumara K, Iyengara NGR, Debb K. Optimum design of laminated composite plates with cutouts using a genetic algorithm. Compos Struct 1998;42(3):265–79.
[14] Tenek LT. Vibration of thermally stressed composite plates with and without cutouts. AIAA J 2000;38(7):1300–1.
[15] Liu Y, Jin F, Li Q. A strength-based multiple cutout optimization in composite plates using fixed grid finite element method. Compos Struct 2006;73(4):403–12.
[16] Dhanaraj R, Palanininathan. Free vibration of initially stressed composite laminates. J Sound Vib 1990;142(3):365–78.
[17] Chen C-S, Cheng W-S, Chien R-D, Doong J-L. Large amplitude vibration of an initially stressed cross ply laminated plates. Appl Acoust 2002;63(9):939–56.
[18] Nayak AK, Moy SSJ, Shenoi RA. A higher order finite element theory for buckling and vibration analysis of initially stressed composite sandwich plates. J Sound Vib 2005;286(4–5):763–80.
[19] Chakrabarti A, Topdar P, Sheikh AH. Vibration of pre-stressed laminated sandwich plates with interlaminar imperfections. J Vib Acoust, ASME 2006;128(6):673–81.
[20] Bert CW. Literature review – research on dynamic behavior of composite and sandwich plates – V: Part II. Shock Vib Dig 1991;23(7):9–21.
[21] Abrate S. Optimal design of laminated plates and shells. Compos Struct 1994;29(3):269–86.
[22] Topal U, Uzman U. Optimal design of laminated composite plates to maximize fundamental frequency using MFD method. Struct Eng Mech 2006;24(4):479–91.
[23] Schmit LA. Structural synthesis – its genesis and development. AIAA J 1981;19(10):1249–63.
[24] Narita Y. Layerwise optimization for the maximum fundamental frequency of laminated composite plates. J Sound Vib 2003;263(5):1005–16.
[25] Hu H-T, Wang K-L. Vibration analysis of rotating laminated cylindrical shells. AIAA J 2007;45(8):2051–61.
[26] Vanderplaats GN. Numerical optimization techniques for engineering design with applications. McGraw-Hill; 1984 [chapter 2].
[27] Haftka RT, Gürdal Z, Kamat MP. Elements of structural optimization. 2nd revised ed. Kluwer Academic Publishers; 1990 [chapter 4].
[28] Hu H-T, Chen J-M. Maximization of fundamental frequencies of axially compressed laminated curved panels against fiber orientation. CMC: Comput Mater Continua 2012;28(3):181–211.
[29] Abaqus, Inc. Abaqus analysis user's manuals and example problems manuals, version 6.11, Providence, Rhode Island; 2011.
[30] Whitney JM. Shear correction factors for orthotropic laminates under static load. J Appl Mech 1973;40(1):302–4.
[31] Cook RD, Malkus DS, Plesha ME, Witt RJ. Concepts and applications of finite element analysis. 4th ed. John Wiley & Sons Inc.; 2002.
[32] Peng H-W. Optimization of fundamental frequencies of axially compressed laminated curved panels with central circular cutouts. M.S. thesis, Department of Civil Engineering, National Cheng Kung University, Tainan, Taiwan, ROC; 2010.